

Influence of B-site chemical ordering on the dielectric response of the $\text{Pb}(\text{Sc}_{1/2}\text{Nb}_{1/2})\text{O}_3$ relaxor

This article has been downloaded from IOPscience. Please scroll down to see the full text article.

2001 J. Phys.: Condens. Matter 13 10231

(<http://iopscience.iop.org/0953-8984/13/45/310>)

View [the table of contents for this issue](#), or go to the [journal homepage](#) for more

Download details:

IP Address: 171.66.16.226

The article was downloaded on 16/05/2010 at 15:07

Please note that [terms and conditions apply](#).

Influence of B-site chemical ordering on the dielectric response of the $\text{Pb}(\text{Sc}_{1/2}\text{Nb}_{1/2})\text{O}_3$ relaxor

C Perrin¹, N Menguy², O Bidault³, C Y Zahra⁴, A-M Zahra⁴,
C Caranoni¹, B Hilczer⁵ and A Stepanov¹

¹ Laboratoire L2MP, UMR 6137—CNRS, Université Aix-Marseille III, Case 151, Faculté des Sciences et Techniques de Saint Jérôme, F-13397 Marseille Cedex 20, France

² Laboratoire de Minéralogie—Cristallographie, UMR 7590 CNRS, Universités Paris 6 et Paris 7, Institut de Physique du Globe, case 115, 4 place Jussieu, 75252 Paris cedex 05, France

³ Laboratoire de Physique, UMR CNRS 5027 Université de Bourgogne, BP 47870, F-21078 Dijon Cedex, France

⁴ Laboratoire TECSEN, UMR 6122—CNRS, Université Aix-Marseille III, Case 151, Faculté des Sciences et Techniques de Saint Jérôme, F-13397 Marseille Cedex 20, France

⁵ Institute of Molecular Physics, Polish Academy of Sciences, Smoluchowskiego 17, PL-60176 Poznan, Poland

E-mail: menguy@lmcp.jussieu.fr and perrin@l2mp.u-3mrs.fr

Received 6 August 2001, in final form 10 September 2001

Published 26 October 2001

Online at stacks.iop.org/JPhysCM/13/10231

Abstract

The influence of chemical B-site ordering between Sc^{3+} and Nb^{5+} cations on the properties of the $\text{Pb}(\text{Sc}_{1/2}\text{Nb}_{1/2})\text{O}_3$ (PSN) relaxor has been investigated. Depending of the degree of ordering, PSN exhibits different behaviours. For a completely disordered material, a relaxor–ferroelectric phase transition is observed at 379 K by DSC. Ordering between Sc^{3+} and Nb^{5+} cations on the B-site of the perovskite structure leads to a non-homogeneous material constituted of two phases: ordered and disordered phases. The phase transition temperature of the ordered phase is confirmed to be lower (346 K) than that of the disordered phase. It appears that the phase transition of the disordered phase is shifted to lower temperature owing to the presence of the ordered phase.

Moreover, an additional short-range structural ordering is shown to exist in disordered PSN. This additional ordering, for which antiparallel displacements of Pb atoms could be involved, is favoured by chemical ordering between Sc^{3+} and Nb^{5+} and is long range in ordered PSN.

1. Introduction

Numerous mixed oxide systems such as complex perovskites $\text{A}(\text{B}'_x, \text{B}''_{1-x})\text{O}_3$, with heterovalent B-site ions, exhibit relaxor behaviour and the study of these materials is of both fundamental and technological interest [1]. The relaxors present diffuse and frequency-dependent dielectric anomaly with high dielectric permittivity values. In such materials, the temperature (T_{max}) and the height of the dielectric permittivity maximum plotted as a function of temperature depend

on the frequency of the applied field. T_{\max} shifts to lower temperatures when the frequency decreases. Moreover, the random mean square value of dielectric polarization persists at temperatures 200–400 K above the dielectric anomaly. Numerous models are proposed to account for the relaxor behaviour: diffuse phase transition [2], superparaelectric [1, 3] and dipolar glass models [4], random-field frustrated ferroelectric [5, 6], interacting polar clusters [7, 8] and spherical random bond-random field models [9]. A mixed ferroglass phase with coexistence of long and short range order is also proposed as the model for description of the 1:1 family relaxors [10].

The 1:1 type ferroelectric relaxors $\text{Pb}(\text{Sc}_{1/2}\text{Nb}_{1/2})\text{O}_3$ and $\text{Pb}(\text{Sc}_{1/2}\text{Ta}_{1/2})\text{O}_3$ (denoted as PSN and PST, respectively) are of special interest because the degree of ordering of B' and B'' type ions can be controlled by thermal treatment [11–16] and they undergo a spontaneous relaxor-ferroelectric transition on cooling [17, 18]. PSN and PST can exist in a disordered state, in which the B' and B'' atoms are statistically distributed on the B-site of the cubic perovskite lattice, or in a long-range ordered state in which the B' and B'' cations occupy alternatively B-sites along the $\langle 111 \rangle$ directions. The ordering can be partial or complete and is evidenced by the presence of superstructure lines in the x-ray diffraction pattern. It should be stressed however, that the heterogeneity of ferroelectric relaxors is rather more complex: besides the above-described chemical order of B-type ions, the material is also considered to contain reorientable dynamic polar clusters in the polarizable matrix [1].

The influence of the B-site ordering on the physical properties of PSN has been studied repeatedly. For Stenger and Burggraaf [12, 13], disordered PSN exhibits a ferroelectric–paraelectric phase transition in a 373 K to 382 K temperature interval. The partially ordered material is constituted of two phases, the ordered phase and the disordered phase, which exhibit a phase transition at about respectively 348 K and 378 K. These results are confirmed by Malibert *et al* [16] and Takesue *et al* [19]. Chu *et al* show that the phase transition observed at 379 K for disordered PSN is a spontaneous first order relaxor-ferroelectric phase transition [18]. Jang and Kim [15] observe the phase transition of the disordered phase at around 378 K. From experiments performed on a PSN ceramic annealed at 1500 K for 5 days, they interpret a discontinuous change in the dielectric permittivity and a DSC peak observed at 348 K as resulting from a relaxor–ferroelectric phase transition of short range ordered PSN. For the same ceramic, they also suggest the existence of a disordered matrix containing small ordered domains that exhibits a continuous ferro–paraelectric transition at about 360 K. In contradiction with these cited above are the results on the influence of Sc/Nb ordering based on the first principles approach by Hemphill *et al* [20]. They concluded that ordered PSN exhibits a normal ferroelectric phase transition at 500 K, i.e. a temperature significantly higher than the relaxor ferroelectric phase transition temperature of disordered PSN.

As the influence of B-site ordering on the physical properties of 1:1 type ferroelectric relaxors is still unclear, this paper is devoted to detailed studies of the relationship between the chemical ordering of Sc^{3+} and Nb^{5+} cations and the dielectric response and thermal properties of PSN ceramics. We report results of dielectric, thermodynamic and structural investigations performed on PSN ceramics with different degrees of order. A particular attention was turned towards the relation between the microstructure of the materials and their properties.

2. Experiment

2.1. Sample preparation

Stoichiometric PSN ceramics were prepared with different degrees of order: (i) highly ordered, (ii) highly disordered and (iii) partially ordered materials.

At each step, precautions were taken in order to avoid lead vacancies in the samples because it has been shown that lead vacancies can entail dramatic modifications of dielectric properties of PSN [18]. This point is very sensitive for PSN because the changes of dielectric properties induced by lead vacancies are similar to those induced by $\text{Sc}^{3+}/\text{Nb}^{5+}$ chemical ordering: the value of the dielectric permittivity is significantly decreased and the phase transition temperature is lowered.

Ceramics were synthesized from a $\text{Pb}(\text{Sc}_{1/2}\text{Nb}_{1/2})\text{O}_3$ powder prepared by the wolframite-type precursor method [21]. Sc_2O_3 and Nb_2O_5 oxides were carefully mixed and calcined in a platinum crucible at 1550 K for 4 hours to form the ScNbO_4 precursor phase; the purity of the obtained ScNbO_4 phase was controlled using x-ray diffraction analysis. Then, the ScNbO_4 phase was mixed with PbO (with an excess amount of PbO equal to 2%) and calcined at 1273 K for 4 hours and afterwards rapidly cooled to room temperature to obtain the $\text{Pb}(\text{Sc}_{1/2}\text{Nb}_{1/2})\text{O}_3$ powder.

Pellets of 6 mm diameter and 0.7 mm thickness were pressed without binder and sintered in an annealing capsule in a similar way to that used by Stenger and Burggraaf [12] in order to prevent PbO losses. Pellets were covered with PSN powder and the crucible was then placed in an alumina crucible containing $\text{PbZrO}_3 + 5\%$ PbO powder to provide a saturated atmosphere with lead oxide.

To obtain the disordered PSN sample (called PSN-00 hereafter), the ceramic sintering was carried out at 1700 K for 20 min and the specimen was then air quenched. Another series of two samples (PSN-60 and PSN-85 hereafter) was prepared with a sintering temperature equal to 1520 K for 4 hours. An extra annealing at 1270 K for 42 hours was performed on PSN-85 in order to obtain a highly-ordered ceramic. All those annealing treatments were carried out using the annealing capsule mentioned above.

X-ray diffraction analysis, performed on each specimen, revealed the existence of small quantities of secondary phases resulting from PbO evaporation, such as pyrochlore and ScNbO_4 phases. These secondary phases were totally removed after a careful and symmetrical polishing of the two sides of each ceramic. The purity of the final pellets of PSN was checked by x-ray diffraction experiments: no supplementary reflection that could be attributed to any secondary phase was detected.

In order to quantify the possible lead deficiency in the samples, the three PSN ceramics were analysed by wavelength dispersive spectroscopy (WDS) on a CAMECA SX50 electron microprobe analyser, using PbO , Sc_2O_3 and Nb_2O_5 oxides for calibration. Analysis of several parts of the polished pellets of PSN reveals a very slight lead excess. It can be concluded from these results that the samples are stoichiometric. Even if there is Pb loss in the superficial layers of the initial ceramics, their core remains stoichiometric. The pellet compacity was more than 95%.

2.2. Experimental techniques

2.2.1. X-ray diffractometry. X-ray diffraction experiments were performed using a Philips X'Pert MPD powder diffractometer equipped with an Anton Paar TTK 450 temperature camera and a $\text{Cu K}\alpha$ diffracted beam graphite monochromator. The evolution of the diffraction pattern as a function of the temperature was studied in the [298 K–408 K] range with 5 K steps. The sample was placed in a dedicated sample holder and the sample surface temperature was controlled in a separate temperature cycle.

2.2.2. Dielectric measurements. The dielectric response of the PSN ceramic samples of various degrees of order was studied in the frequency range from 100 Hz to 100 kHz and in the

temperature range 320–420 K. The capacitance and dielectric losses were measured by means of a computer controlled HP4284A precision *LCR*-meter in a low electric field strength of 1 kV m^{-1} . The temperature was changed at a rate of 0.5 K min^{-1} . Thermally stimulated depolarization current (TSDC) measurements were carried out on a Keithley electrometer following a zero field heating after field cooling protocol (ZFH–FC), with a heating rate of 0.5 K min^{-1} and an applied field strength equal to 1 kV cm^{-1} . In this case, the conductivity can be neglected.

2.2.3. Differential scanning calorimetry. Differential scanning calorimetry experiments were performed using a Perkin–Elmer 1020 with a heating rate equal to 20 K min^{-1} . Each pellet was placed into an alumina crucible and the calibration of the calorimeter was done using pure indium melting.

2.2.4. Transmission electron microscopy. Transmission electron microscopy (TEM) was carried out using a JEOL 2010F electron microscope. Fragments of the ceramics were crushed in an agate mortar and then deposited on carbon film. Selected area electron diffraction patterns (SAEDs) were obtained using a very low excitation condenser lens in order to avoid sample irradiation damage.

3. Results

3.1. Degree of order

At room temperature, the structure of disordered PSN is rhombohedral (space group $R3m$) [16, 22, 23] with $a_{rh} = 4.0828(1) \text{ \AA}$ and $\alpha_{rh} = 89.915(2)^\circ$ [23]. In the case of lead scandium tantalate (PST), it has been shown that the ordering between B' and B'' cations induces the appearance of superstructure reflections and the ordered phase is still rhombohedral with the $R3$ space group [24]. The x-ray diffraction results obtained on the three studied ceramics indicate that the positions of the peaks are compatible with the $R3m$ space group over the whole diffraction pattern. Nevertheless, for PSN-60 and PSN-85, a careful examination of the diffraction pattern reveals the existence of one weak reflection related to the Sc/Nb ordering.

The degree of order of our PSN ceramics was estimated from the comparison of the integrated intensities of the superstructure reflection and the adjacent fundamental reflection following a method previously used for partially ordered PST with the $Fm\bar{3}m$ space group [12, 25]. For rhombohedral ordered PSN, the superstructure peak splitting due to the rhombohedral distortion is almost indistinguishable and the method can also be applied. The main problem related to the determination of the degree of order of PSN ceramics lies in the weakness of the superstructure reflection intensity: for a completely-ordered structure, the theoretical intensity ratio I_{111}/I_{200} is equal to 0.09. For each sample, measurements of the superstructure reflection (indexed 111_F in the pseudo-cubic cell of parameter $2 a_{rh}$) and the fundamental reflection 200_F were performed and the corresponding integrated intensities were extracted, using the Profile SOCABIM software. The results are summarized in table 1.

The PSN-00 sample is considered as disordered since no superstructure reflection is visible by x-ray diffraction resolution.

The analysis of the peak widths shows that for the ordered PSN-85, the full width at half maximum (FWHM) of the superstructure reflection ($0.081^\circ - 2\theta$ at $2\theta \approx 18.8^\circ$) is slightly lower than the FWHM of the fundamental peak ($0.088^\circ - 2\theta$ at $2\theta \approx 21.8^\circ$). This result indicates that the mean size of the ordered domains is of the same order of magnitude compared to the size of the PSN coherent diffracting domains.

Table 1.

	PSN-00	PSN-60	PSN-85
Sintering	1700 K/20 min PbZrO ₃ + PbO	1520 K/4 hours PbZrO ₃ + PbO	1520 K/4 hours PbZrO ₃ + PbO
Annealing temperature/time	—	—	1270 K/42 hours
Composition	[Pb] _{at} = 19.9 ± 0.2 [Sc] _{at} = 9.8 ± 0.2 [Nb] _{at} = 10.2 ± 0.2	[Pb] _{at} = 20.0 ± 0.35 [Sc] _{at} = 9.5 ± 0.2 [Nb] _{at} = 9.9 ± 0.3	[Pb] _{at} = 20.7 ± 0.35 [Sc] _{at} = 9.6 ± 0.3 [Nb] _{at} = 10.1 ± 0.2
Degree of order s			
$s = \left[\frac{I_{111}}{I_{200}} \right]_{exp}^{1/2} / \left[\frac{I_{111}}{I_{200}} \right]_{theo}^{1/2}$	$s = 0$ disordered	$s \approx 0.6$ partially ordered	$s = 0.85$ majority ordered

For PSN-60, the FWHM of the superstructure reflection is larger than that of the fundamental peak. For this sample, the size of the ordered domains seems to be smaller than for the highly-ordered PSN-85 sample and is roughly estimated, from the Scherrer's formula and TEM observations, at 50 nm.

3.2. Dielectric properties

Figure 1 shows the real part of permittivity as a function of temperature (heating/cooling) for PSN-00 (a), PSN-60 (b), PSN-85 (c).

As shown in figure 1(a), PSN-00 exhibits strong frequency dispersion and a sharp drop of the dielectric permittivity at a frequency-independent temperature of 383 K on heating. On cooling, this discontinuity of permittivity occurs at 374 K, indicating the existence of a thermal hysteresis. These results are consistent with previous results reported in the literature and are typical of the relaxor to normal ferroelectric phase transition of stoichiometric disordered PSN [13, 15, 16, 18].

For PSN-60 (figure 1(b)), two successive sharp variations, occurring at 350 K and 375 K on heating, are clearly visible (and are observed at respectively 345 K and 366 K on cooling). These results are very similar to those obtained by Stenger and Burggraaf for a partially ordered PSN ceramic whose degree of order was estimated equal to 0.52 [12, 13]. The authors concluded that the two sharp variations they observed at 346 K and 375 K correspond respectively to the ferroelectric-to-paraelectric phase transitions of the ordered phase and the disordered phase of PSN. It can be concluded that the PSN-60 ceramic is constituted of two phases: disordered PSN and ordered PSN. For PSN-85, the temperature dependence of the real part of dielectric permittivity is more difficult to analyse: a frequency dispersion is visible but no sharp drop of the dielectric permittivity can be observed (figure 1(c)). Nevertheless, considering the first derivative function of $\varepsilon(T)$, it is possible to distinguish two slight variations of the dielectric permittivity at 350 K and 369 K on heating (at 345 K and 358 K on cooling).

ZFH-FC depolarization current measurements performed on these samples are shown in figure 2. It can be seen that for PSN-00, a single and sharp signal is observed at 384 K (figure 2(a)).

For PSN-60, two peaks are observed: a sharp peak at 375 K and a broader one at 352 K (figure 2(b)). Two main peaks are visible for PSN-85: a large one at 370 K and a smaller one at 350 K. It can also be noticed that a shoulder is also observed at about 380 K (indicated by an arrow in figure 2(c)).

The TSDC measurements are consistent with the dielectric permittivity studies: to each drop of dielectric permittivity corresponds a depolarization current. The extensive studies of dielectric properties of these samples are reported in another paper [26].

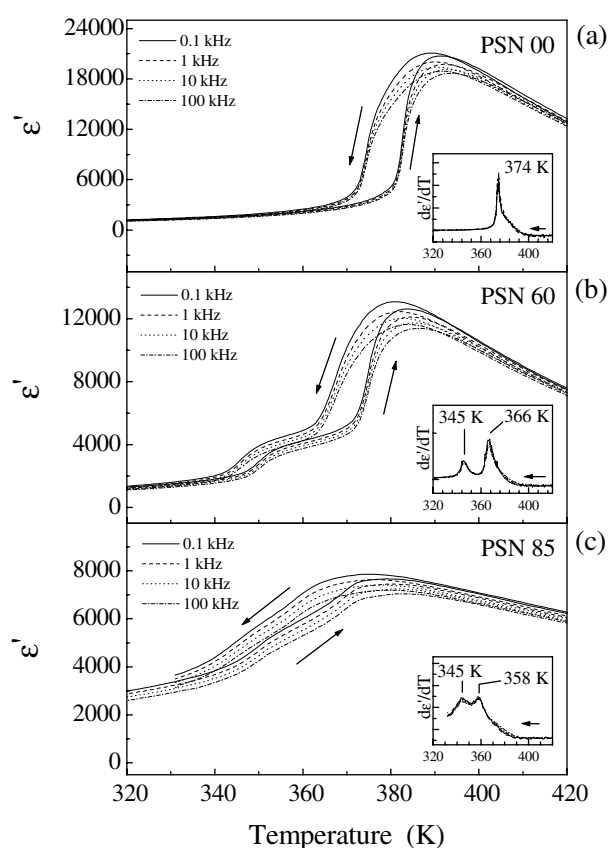


Figure 1. Temperature dependence of the real part of the dielectric permittivity for PSN-00 (a), PSN-60 (b), PSN-85 (c) and for different frequencies. Measurements were performed on cooling and heating. Insert: first derivative of the dielectric permittivity as a function of temperature.

3.3. Differential scanning calorimetry

As shown in figure 3(a), a sharp endothermic peak centred at 379 K is observed for disordered PSN-00 and is consistent with the discontinuity of permittivity and the depolarization current observed at 384 K on heating.

For PSN-60 two endothermic heat effects are clearly observed at 371 K and 347 K in agreement with dielectric measurements (figure 3(b)), whereas for PSN-85 the DSC plot exhibits a major endothermic peak at 346 K, a small peak centred at 366 K and a slight shoulder at about 376 K (figure 3(c)).

The sharpness of the endothermic peak observed at 379 K for PSN-00 indicates that the disordered phase of this ceramic is homogeneous, unlike PSN-60 and PSN-85, for which broader peaks are observed.

For each sample, there is a systematic and constant shift between transition temperatures deduced from DSC experiments and dielectric measurements. These apparent discrepancies are essentially due to the difference between the heating rates used in the different methods. Hence, the DSC measurements confirm the results obtained from the dielectric experiments: as the degree of chemical order increases, the magnitude of the heat effect observed at 346 K increases and the phase transition temperature of the disordered phase is shifted to lower temperature.

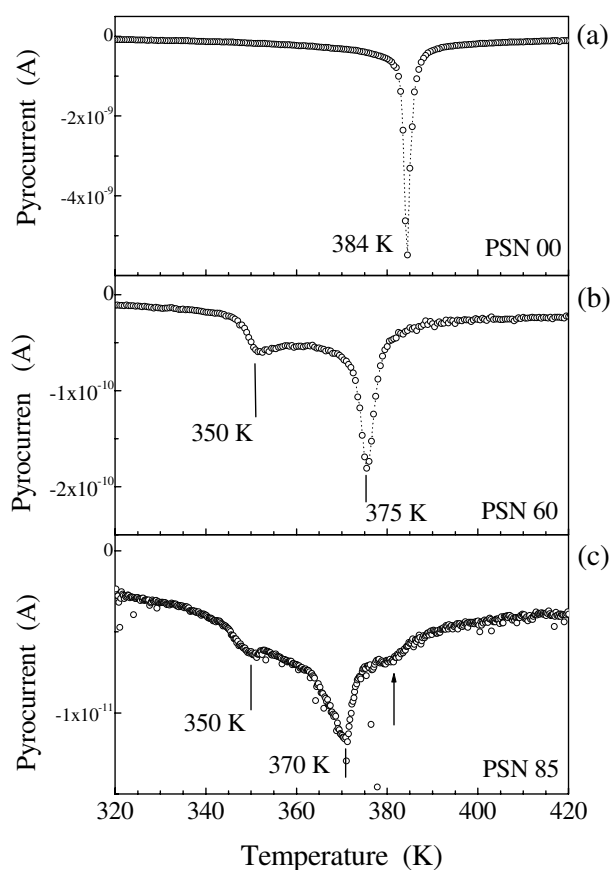


Figure 2. Pyroelectric current recorded following a 'zero field heating after field cooling' protocol with an applied field strength equal to 1 kV cm^{-1} for PSN-00 (a), PSN-60 (b) and PSN-85 (c).

3.4. X-ray diffraction experiments

The existence of structural phase transitions in the three ceramics was confirmed by *in situ* x-ray experiments. As shown in figure 4, the splitting of the 220_{cub} (indexed in the primitive cell) reflection due to the rhombohedral distortion occurs at about 380 K for PSN-00 and 375 K for PSN-60. For PSN-00, this splitting corresponds unambiguously to the relaxor–ferroelectric phase transition. In the case of PSN-60, only the phase transition of the disordered phase can be seen; the phase transition of the ordered part does not induce a measurable broadening. This is due to the fact that the parameters of both ordered and disordered phases are very close and is also due to the presence of the $K\alpha$ doublet. Due to the 5 K step used for this experiment, the transition temperature is not precisely known. Nevertheless, it can be seen that the phase transition temperature of disordered PSN is lower for the partially ordered PSN-60 ceramic than for the completely-disordered PSN-00 ceramic.

For PSN 85, the transition temperature was determined from the broadening of the 220 reflection: a strong variation of the FWHM, due to the rhombohedral splitting, is observed around 350 K. For this sample, the small variation of the FWHM observed for a temperature above 360 K is probably caused by the contribution of the rhombohedral phase of the persistent disordered PSN.

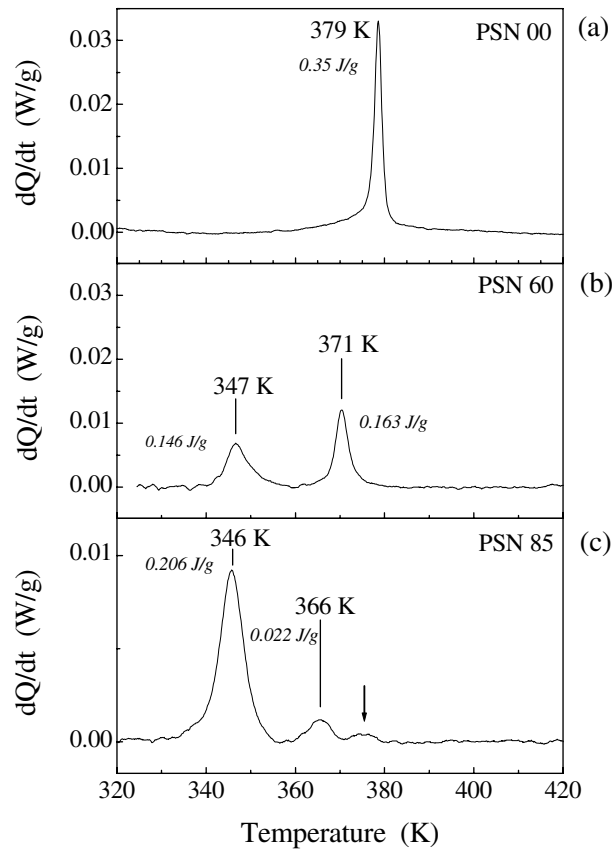


Figure 3. DSC curves obtained for the three samples PSN-00 (a), PSN-60 (b) and PSN-85 (c). For each peak, the magnitude of the heat effect is indicated in italics.

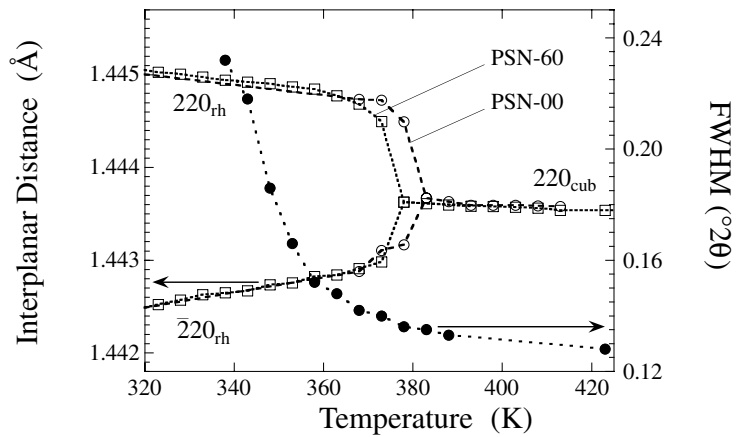


Figure 4. Temperature dependence of structural parameters. For the PSN-00 and PSN-60 ceramics, the variation of the 220 interplanar distance is reported. For the PSN-85 ceramic the evolution of the FWHM of the 220 peak versus temperature is plotted.

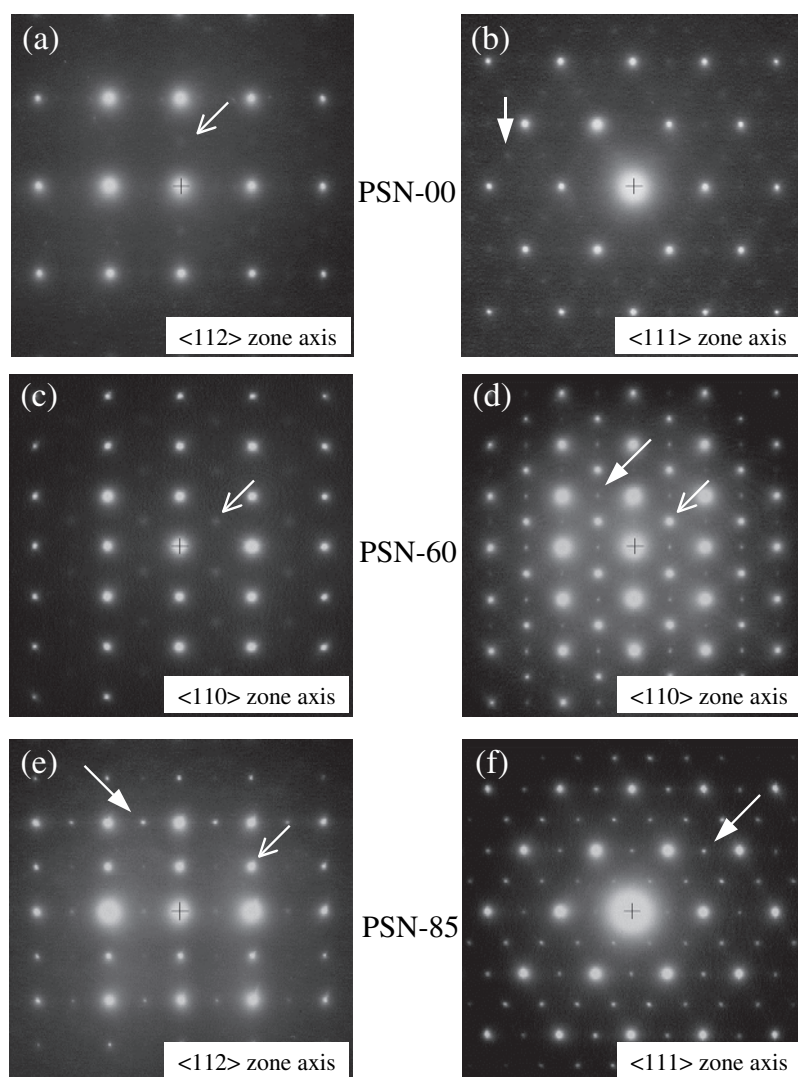


Figure 5. SAED patterns of PSN obtained at room temperature for PSN-00 (a) and (b), PSN-60 (c) and (d), PSN-85 (e) and (f). The $h + \frac{1}{2}k + \frac{1}{2}l + \frac{1}{2}$ superstructure reflections due to the Sc/Nb chemical ordering are indicated by open arrows. The $h + \frac{1}{2}k + \frac{1}{2}0$ are indicated by full arrows.

3.5. Transmission electron microscopy

Dielectric measurements, thermal analyses and x-ray diffraction experiments suggest the existence of at least two different phases of PSN in the various studied samples: chemically-ordered and disordered phases. In order to confirm such hypotheses, TEM experiments were carried out on the samples. Representative SAED patterns obtained from the three samples are shown in figure 5. The SAED patterns related to the three samples differ in the intensity of the superstructure reflections superimposed on the fundamental Bragg peaks. Two kinds of superstructure reflections are detected. $h + \frac{1}{2}k + \frac{1}{2}l + \frac{1}{2}$ superstructure reflections are due to the chemical ordering between Sc^{3+} and Nb^{5+} cations and are visible on $\langle 112 \rangle$ and $\langle 110 \rangle$

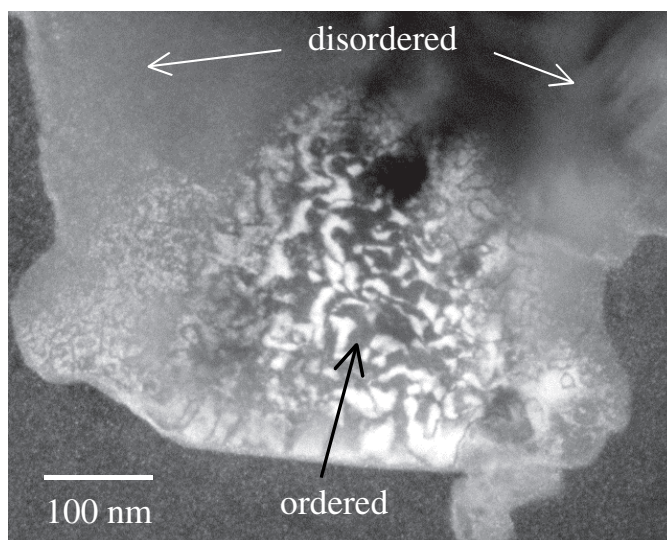


Figure 6. Dark field image of a fragment of the PSN-60 ceramic showing the coexistence of ordered and disordered areas in the same grain. The ordered areas are characterized by the presence of antiphase domain boundaries (APBs) whereas these APBs are not visible in disordered areas.

zone axis SADPs. $h + \frac{1}{2}k + \frac{1}{2}0$ superstructure reflections are also observed and are visible along all zone axis SADPs. This type of reflection has already been observed in PST, PSN and PZT and hypotheses of antiparallel (or antiferroelectric) displacements of Pb atoms or B-site cations have been proposed in order to explain this additional ordering [23, 27–33].

For PSN-00, $h + \frac{1}{2}k + \frac{1}{2}l + \frac{1}{2}$ superstructure reflections are found to be very weak (figure 5(a)) despite the long exposure time used; this observation is consistent with the x-ray diffraction results. Moreover, in agreement with high resolution electron microscopy (HREM) observations, the diffuseness of these reflections indicates that the chemical ordering is at very short range (few cells). Very weak $h + \frac{1}{2}k + \frac{1}{2}0$ superstructure reflections are also visible in the $\langle 111 \rangle$ zone axis SAED pattern (figure 5(b)).

For the PSN-60 ceramic, two kinds of PSN region are found: some regions for which both types of superstructure reflection are weak and diffuse as in PSN-00 (figure 5(c)) and some for which both types of superstructure reflection are strong and well defined (figure 5(d)). In the latter case, the most frequently observed microstructure consists of disordered areas near ordered regions in the same crystallites as shown in figure 6. In this dark field image obtained with the $\frac{1}{2} \frac{1}{2} \frac{1}{2}$ superstructure reflection, antiphase domain boundaries are clearly visible in the ordered region, whereas they are not visible in disordered regions. The contrast of the ordered regions indicates that the degree of order is high and homogeneous in these ordered areas. Concerning the disordered regions, the interpretation of the observed contrast is not straightforward. Some bright dots are visible and could be interpreted as small ordered domains dispersed in the disordered matrix but this hypothesis is somewhat speculative. The corresponding SADP of such a disordered region (figure 5(c)) indicates that chemical ordering is short range (a few cells), as for PSN-00. From the selected aperture diameter, the size of the homogeneous disordered regions can be estimated to be equal to at least 100 nm. These TEM results confirm the coexistence of ordered and disordered phases of PSN within the PSN-60 ceramic.

Almost all of the SADPs obtained on PSN-85 exhibit well defined, strong $h + \frac{1}{2}k + \frac{1}{2}l + \frac{1}{2}$ and also $h + \frac{1}{2}k + \frac{1}{2}0$ superstructure reflections as shown in figures 5(e) and 5(f). It can be concluded that for PSN-85, the corresponding orderings are both long range.

From these TEM observations, it can be concluded that

- (i) PSN-00 is homogeneous and disordered;
- (ii) PSN-60 is constituted of two phases, disordered and ordered phases of PSN;
- (iii) PSN-85 is almost completely ordered;
- (iv) the occurrence of $h + \frac{1}{2}k + \frac{1}{2}0$ superstructure reflections is strongly correlated to the chemical ordering between Sc^{3+} and Nb^{5+} cations: the more chemically-ordered the sample is, the more intense and well defined $h + \frac{1}{2}k + \frac{1}{2}0$ superstructure reflections are.

4. Discussion

4.1. Influence of chemical ordering

The first point of the discussion concerns the influence of the chemical order between Sc^{3+} and Nb^{5+} cations on the dielectric properties of PSN. The results reported in this paper clearly show that the chemical ordering between Sc^{3+} and Nb^{5+} cations induces a lowering of the relaxor-to-ferroelectric transition temperature.

When the chemical ordering is long range within the sample, we confirm the results of Stenger and Burggraaf [12, 13] and Malibert *et al* [16] for which the phase transition temperature of the ordered phase equal to 346 K is reported. In contrast, our results disagree with recent theoretical results on the influence of chemical ordering on the properties of ordered and disordered PSN [20] in which the phase transition temperature in ordered PSN is reported to be significantly higher than in disordered PSN.

As previously shown by Stenger and Burggraaf and recently by Blinc *et al* [34], our results also confirm that the chemical ordering yields to a non-spatially homogeneous material constituted of disordered and ordered phases. Moreover, the present results show that the phase transition temperature of the disordered phase is lowered due to the presence of the ordered phase. For instance, whatever the experimental method used, the PSN-00 ceramic, which is free of ordered domains, exhibits a phase transition temperature at about 8 K higher than the disordered phase of the ceramic PSN-60.

DSC experiments were performed on the starting PSN powder from which all the ceramics were prepared. As shown in figure 7, the corresponding DSC curve is clearly characterized by two thermal effects whose peaks are centred at respectively 372 K and 383 K on heating (361 K and 371 K on cooling but not shown). It can be noticed that the peaks deduced from the fit procedure are somewhat broadened when compared to those obtained from the ceramics. Hence, the PSN powder seems to be constituted of two phases exhibiting a phase transition respectively at about 370 K and 380 K. This result suggests that a part of the PSN powder contains ordered domains that decrease the phase transition temperature of the disordered phase.

TEM observations were carried out in order to investigate the microstructure of the PSN powder. Two kinds of PSN material are found: some homogeneously-disordered crystallites characterized by very weak superstructure reflections (as in the PSN-00 ceramic) and some crystallites containing simultaneously disordered areas and partially ordered regions. Figure 8 displays a $[112]$ zone-axis high resolution electron microscope (HREM) image of such partially-ordered crystallite. In the ordered region (labelled O), the periodicity along the $[111]$ direction is doubled. For the corresponding thickness and defocus conditions of this image, the

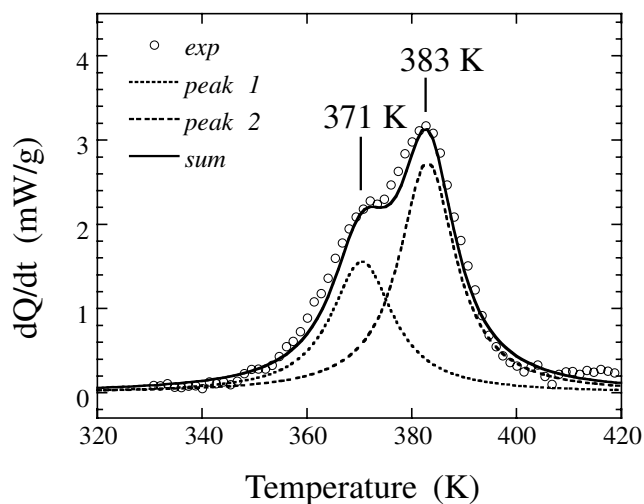


Figure 7. DSC curve obtained on the PSN powder. Two distinct thermal effects are visible. The double peak was fitted using two Cauchy functions.

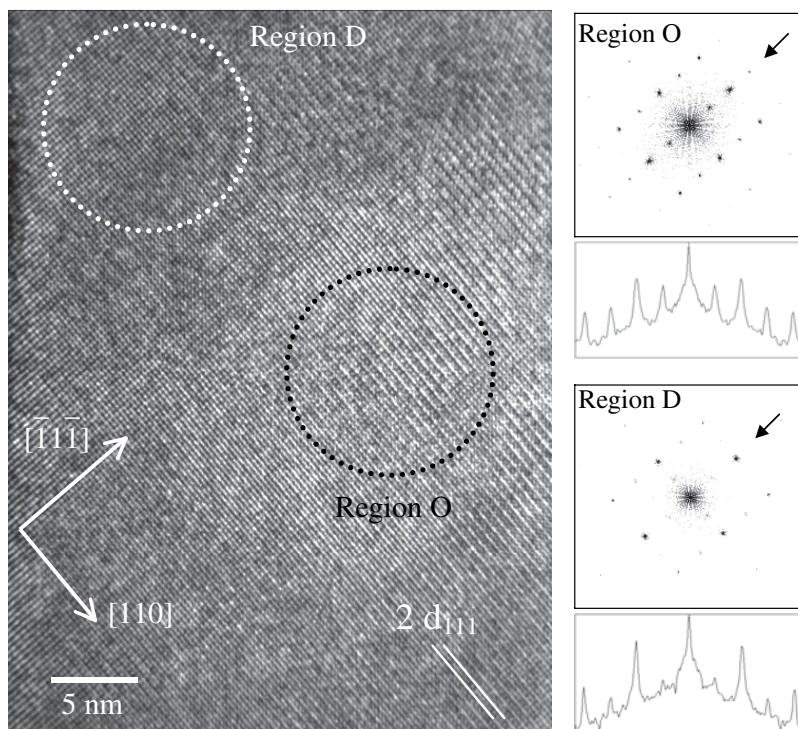


Figure 8. HRTEM image of a grain of the PSN starting powder with the incident electron beam along the $[\bar{1}12]$ direction. Ordered domains (region O) are characterized by an enhancement of the fringes perpendicular to the $[111]$ direction with a doubling periodicity. This doubled periodicity is not observed for the adjacent disordered region (region D).

For each region, the corresponding FFTs are reported with an intensity profile along the $[111]^*$ reciprocal direction (indicated by an arrow).

chemical ordering is expressed by a brightness enhancement of the fringes perpendicular to the [111] direction with a doubling periodicity. This ordered region is surrounded by a disordered matrix (labelled D) for which no doubling periodicity is observed. The individual fast Fourier transforms related to each region are also shown. For the ordered region, $h + \frac{1}{2}k + \frac{1}{2}l + \frac{1}{2}$ superstructure reflections are clearly visible, whereas for the disordered regions the intensity of the superstructure reflections is significantly lower (the power spectrum is displayed using a logarithmic scale) indicating the existence of a very short-range order (a few cells). From the analysis of several HREM images, it appears that the mean size of ordered regions is in the range 5–10 nm.

Since it is impossible to estimate the total number of ordered domains dispersed in the whole sample from TEM images, x-ray diffraction experiments were carried out on the PSN powder using a long counting time. No superstructure reflection, even broadened, was observed. It can be concluded that these ordered domains represent a small fraction of the material.

The formation of these small chemically-ordered domains could have occurred during the cooling from 1273 K to room temperature. This hypothesis is corroborated by the fact that the PSN-00 ceramic, which was air quenched, does not exhibit any ordered domains.

From DSC and TEM studies, it appears then that the starting PSN powder is a mixture of two phases: a homogeneous disordered phase exhibiting a transition at about 380 K and a heterogeneous disordered phase for which a phase transition is observed at about 370 K and containing small ordered regions, whose size is in the range 5–10 nm. From the absence of any phenomenon occurring at 346 K (e.g. related to the phase transition of the ordered phase), it can be concluded that, probably due to their small size, the ordered domains do not behave like the bulk-ordered phase. Nevertheless, the influence of these small ordered regions on the disordered phase of PSN is clearly evidenced: dispersed within the disordered PSN matrix, they lower the relaxor–ferroelectric phase transition temperature of disordered PSN.

According to this model, the phenomenon expressed by a small shoulder visible at 380 K on the TSDC curve (figure 2(c)) and a small endothermic effect at 376 K (figure 3(c)) for the ceramic PSN-85, corresponds to the phase transition of a disordered phase containing a lower concentration of ordered regions than the disordered phase for which the phase transition is observed 10 K lower. The mechanisms involved in the lowering of the phase transition of the disordered phase by the presence of small ordered domains remains to be determined. A possible explanation lies in a ferroelastic interaction between ordered domains and the surrounding disordered matrix. As recently reported for PMN [35], the compositional fluctuation and lattice strain lying at the boundary between ordered domains and the disordered matrix could play an important role in the formation of polar clusters.

4.2. Hypothesis of lead vacancies

A possible influence of lead vacancies in our samples that could explain the results has to be dismissed. Firstly, the compositional analyses reveal that, instead of Pb loss, a slight Pb excess is rather observed. Furthermore, the behaviour of the PSN-00 ceramic, annealed at high temperature, is the same as that reported for stoichiometric disordered PSN in [18]. For PSN-60 and PSN-85 ceramics, a lowering of the phase transition temperature is evidenced for the disordered phase, but the phase transition temperature of the ordered phase does not change. When they exist, the Pb vacancies are supposed to inhibit the long range dipole coupling and to smear the transformation in disordered PSN. It is reasonable to assume that the same effect has to be observed in ordered PSN, whereas this is not observed in our results.

Finally, in order to test the lead loss, the PSN-60 ceramic has been re-annealed in a PbO-rich atmosphere at 1020 K for 12 hours. This temperature is low enough that the annealing does not induce a subsequent change in the cation ordering but high enough to favour the pick-up of any missing lead. Neither weight gain nor significant changes in its dielectric response have been observed.

4.3. $h + \frac{1}{2}k + \frac{1}{2}0$ superstructure reflections

The $h + \frac{1}{2}k + \frac{1}{2}0$ superstructure reflections were observed in different relaxor compounds such as PMN [36, 37], PST [27, 28, 38], PZT [30, 32] and also in PSN [19, 33, 39, 40].

In the neutron diffraction study of disordered PSN, Perrin *et al* reported the presence of weak $h + \frac{1}{2}k + \frac{1}{2}0$ superstructure reflections at 2 K. However, these reflections were not observed by these authors at and above room temperature. For Takesue and coworkers, a $0 \frac{1}{2} \frac{5}{2}$ superstructure reflection has been observed at 570 K for disordered PSN whereas it has not been observed at 470 K for ordered PSN. Despite the fact that their x-ray diffraction experiments were carried out at high temperature, the results of Takesue *et al* seem to disagree with our present TEM investigations, since at room temperature and for disordered PSN the $h + \frac{1}{2}k + \frac{1}{2}0$ superstructure reflections are almost invisible.

The physical origin of these $h + \frac{1}{2}k + \frac{1}{2}0$ superstructure reflections is still a matter of debate. A frequently proposed model suggests antiparallel shifts of lead atoms in $\langle 100 \rangle_{pc}$ or in $\langle 110 \rangle_{pc}$ pseudo-cubic directions. Such a hypothesis was proposed for PST [27, 38, 41]. For $\text{PbZr}_{1-x}\text{Ti}_x\text{O}_3$ with x close to 0.07, two similar models were proposed. In the latter case, the origin of these superlattice reflections is explained by the existence of local regions presenting antiparallel Pb displacements along $\langle 110 \rangle_{pc}$ [32] or $\langle 100 \rangle_{pc}$ directions [30].

For disordered PSN in the rhombohedral ferroelectric phase, an additional displacement of Pb atoms, perpendicular to the threefold polar axis was proposed [16, 23, 29, 40], but no particular direction of the Pb-shift was unambiguously determined. It is worth noting that in each case, the magnitude of the extra shift is about 0.2 Å.

Finally, it has to be noticed that these models of Pb displacement are very similar to those reported in lead based perovskites such as PbZrO_3 [42, 43] or other B-site ordered perovskite $\text{Pb}_2\text{YbNbO}_6$ [44], $\text{Pb}_2\text{YbTaO}_6$ [45] or Pb_2MgWO_6 [46]. As for these complex perovskites, our TEM observations show clearly the correlation between $\text{Sc}^{3+}/\text{Nb}^{5+}$ chemical ordering and the extra ordering of Pb cations. A similar result was reported by Dkhil for the $\text{PbMg}_{0.3}\text{Nb}_{0.6}\text{Ti}_{0.1}\text{O}_3$ compound [36].

An additional ordering of Pb atoms was suggested to exist at a short-range scale in disordered PSN [16, 23]. The present paper confirms its existence but at a long-range scale in ordered PSN. The exact nature of Pb atom ordering and the origin of the influence of $\text{Sc}^{3+}/\text{Nb}^{5+}$ on this ordering remains to be precised. However, it can be assumed that a possible frustration between this additional ordering of Pb atoms and the ferroelectric ordering plays an important role in the relaxor behaviour of PSN as previously suggested [47].

Acknowledgements

The authors would like to thank Dr Robaut (CMTC, INP Grenoble) and Dr Fialin (CAMPARIS, Université Paris 6) for EMPA analyses and J Martin for making the x-ray diffraction sample holder. We are grateful for the use of the Jeol 2010F TEM provided by the Centre Pluridisciplinaire de Microscopie et de Microanalyse (CP2M) at the University of Aix-Marseille III. We also gratefully thank Professor Vuillaume for his help.

References

- [1] Cross L E 1994 *Ferroelectrics* **151** 305–20
- [2] Smolensky G A 1970 *J. Phys. Soc. Japan* **28** (Supplement) 26
- [3] Cross L E 1987 *Ferroelectrics* **76** 241–67
- [4] Viehland D, Jang S J and Cross L E 1990 *J. Appl. Phys.* **68** 2916
- [5] Westphal V, Kleemann W and Glinchuk M D 1992 *Phys. Rev. Lett.* **68** 847
- [6] Tagantsev A K and Glazounov A E 1998 *Phys. Rev. B* **57** 57
- [7] Vugmeister B E and Rabitz H 1998 *Phys. Rev. B* **57** 7581
- [8] Vugmeister B E and Rabitz H 2000 *Phys. Rev. B* **61** 14 448–52
- [9] Pirc R and Blinc R 1999 *Phys. Rev. B* **60** 13470–78
- [10] Glinchuk M D, Stepanovitch V A, Hilczer B, Wolak J and Caranoni C 1999 *J. Phys.: Condens. Matter* **11** 6263–75
- [11] Setter N and Cross L E 1980 *J. Appl. Phys.* **51** 4356–60
- [12] Stenger C G F and Burggraaf A J 1980 *Phys. Status Solide a* **61** 275–85
- [13] Stenger C G F and Burggraaf A J 1980 *Phys. Status Solide a* **61** 653–64
- [14] Bokov A A and Rayevski I P 1993 *Ferroelectrics* **144** 147
- [15] Jang H M and Kim S C 1997 *J. Mater. Res.* **12** 2117–26
- [16] Malibert C, Dkhil B, Kiat J M, Durand D, Berar J F and Spasojevic-de-Biré A 1997 *J. Phys.: Condens. Matter* **9** 7485–500
- [17] Chu F, Setter N and Tagantsev A K 1993 *J. Appl. Phys.* **74** 5129–34
- [18] Chu F, Reaney I M and Setter N 1995 *J. Appl. Phys.* **77** 1671–76
- [19] Takesue N, Fujii Y, Ichihara M, Chen H, Tatemori S and Hatano J 1999 *J. Phys.: Condens. Matter* **11** 8301–12
- [20] Hemphill R, Bellaiche L, Garcia A and Vanderbilt D 2000 *Appl. Phys. Lett.* **77** 3642–44
- [21] Swartz S L and Shrout T R 1982 *Mater. Res. Bull.* **17** 1245–50
- [22] Knight K S and Baba-Kishi K Z 1995 *Ferroelectrics* **173** 341–49
- [23] Perrin C, Menguy N, Suard E, Muller C, Caranoni C and Stepanov A 2000 *J. Phys.: Condens. Matter* **12** 7523–39
- [24] Woodward P M and Baba-Kishi K Z 1998 *Proc. 11th IEEE Symp. on Applications of Ferroelectrics, ISAF 98 (Montreux)* (Piscataway: NY IEEE) pp 447–50
- [25] Lampin P, Menguy N and Caranoni C 1995 *Phil. Mag. Lett.* **72** 215–22
- [26] Bidault O, Perrin C, Caranoni C and Menguy N 2001 *J. Appl. Phys.* **90** 4115–21
- [27] Randall C A, Barber D J and Whatmore R W 1987 *J. Microsc.* **145** 275–91
- [28] Baba-Kishi K Z and Barber D J 1990 *J. Appl. Crystallogr.* **23** 43–54
- [29] Malibert C 1998 *Thesis* Université de Paris 6
- [30] Corker D L, Glazer A M, Whatmore R W, Stallard A and Fauth F 1998 *J. Phys.: Condens. Matter* **10** 6251–69
- [31] Baba-Kishi K Z 1998 *Proc. 17th Conf. of Applied Crystallography (Wisla)* (Singapore: World Scientific) pp 333–37
- [32] Ricote J, Corker D L, Whatmore R W, Impey S A, Glazer A M, Dec J and Roleder K 1998 *J. Phys.: Condens. Matter* **10** 1767–86
- [33] Takesue N, Fujii Y, Ichihara M and Chen H 1999 *Phys. Lett. A* **257** 195–200
- [34] Blinc R, Gregorovic A, Zalar B, Pirc R, Laguta V V and Glinchuk M D 2001 *J. Appl. Phys.* **89** 1349–54
- [35] Jin H Z, Zhu J, Miao S, Zhang X W and Cheng Z Y 2001 *J. Appl. Phys.* **89** 5048–52
- [36] Dkhil B 1999 *Thesis* Université de Paris 11 Orsay
- [37] Egami T, Dmowski W, Teslic S, Davies P K, Chen I-W and Chen H 1998 *Ferroelectrics* **206–207** 231–44
- [38] Baba-Kishi K Z, Gressey G and Cernik R J 1992 *J. Appl. Crystallogr.* **25** 477–87
- [39] Takesue N, Fujii Y, Ichihara M and Chen H 1999 *Phys. Rev. Lett.* **82** 3709–12
- [40] Perrin C 2000 *Thesis* Université de Aix-Marseille 3
- [41] Reaney I M, Barber D J and Watton R 1992 *J. Mater. Sci.* **3** 51–63
- [42] Glazer A M, Roleder K and Dec J 1993 *Acta Crystallogr. B* **49** 846–52
- [43] Teslic S and Egami T 1996 *Acta Crystallogr. B* **54** 750–65
- [44] Kwon J R and Wong K C 1991 *J. Phys.: Condens. Matter* **3** 2147–55
- [45] Sciau P, Lampis N and Geddo-Lehmann A 2000 *Solid State Commun.* **116** 225–30
- [46] Baldinozzi G, Sciau P and Bulou A 1995 *J. Phys.: Condens. Matter* **7** 8109–17
- [47] Balashova E V and Tagantsev A K 1993 *Phys. Rev. B* **48** 9979–86